ELECTRONIC SUPPLEMENTARY INFORMATION

High-level *ab initio* potential energy surface and dynamics of the $F^- + CH_3I$ S_N2 and proton-transfer reactions

Balázs Olasz, István Szabó,[a] and Gábor Czakó*

Department of Physical Chemistry and Materials Science, Institute of Chemistry, University of Szeged, Rerrich Béla tér 1, Szeged H-6720, Hungary

[a] Present address: Department of Chemistry, King's College London, London SE1 1DB, United Kingdom

* E-mail: gczako@chem.u-szeged.hu

Table S1. Energies (in kcal/mol) relative to the F^- + CH_3I reactants for the stationary points of the FCH_3I^- system at different levels of theory

	aVDZ[a]	aVTZ[b]	aVQZ[c]	ΔCore[d]	ΔZPE[e]	Classical[f]	Adiabatic[g]
HMIN	–19.7	–19.5	–19.3	+0.0	–0.1	–19.3	–19.3
TS1	5.7	5.6	5.8	+0.4	–2.3	6.2	3.9
MIN2	5.2	5.1	5.4	+0.4	–2.0	5.7	3.7
TS2	9.3	8.9	9.0	+0.4	–2.6	9.4	6.8
MIN3	4.8	4.7	5.0	+0.3	–2.0	5.3	3.3
TS1'	6.5	6.6	6.8	+0.5	–2.1	7.3	5.2
MIN2'	4.5	4.7	4.9	+0.5	–1.5	5.4	3.9
TS2'	5.9	6.0	6.2	+0.4	–2.3	6.6	4.3
FSMIN	–22.6	–22.8	–22.7	+0.5	–0.1	–22.1	–22.2
PREMIN	–17.3	–17.4	–17.3	+0.1	+0.1	–17.2	–17.1
POSTMIN	–55.2	–54.9	–55.4	+0.6	+2.0	–54.8	–52.8
HTS	–16.8	–16.8	–16.6	+0.0	+0.0	–16.6	–16.6
DITS	8.4	8.6	8.8	+0.2	–2.0	9.1	7.0
WALDENTS	–17.1	–17.3	–17.2	+0.2	+0.0	–17.0	–17.0
FSTS	19.9	19.5	19.6	+0.5	–0.4	20.1	19.8
$CH_3F + I^-$	–47.4	–47.3	–47.8	+0.8	+1.8	–46.9	–45.2
$CH_2I^- + HF$	19.0	18.8	18.7	+0.6	–3.5	19.4	15.9

[a] CCSD(T)-F12b/aug-cc-pVDZ-PP, where -PP denotes ECP and the corresponding aug-cc-pVDZ-PP basis for I.

[b] CCSD(T)-F12b/aug-cc-pVTZ-PP, where -PP denotes ECP and the corresponding aug-cc-pVTZ-PP basis for I.

[c] CCSD(T)-F12b/aug-cc-pVQZ-PP energies at the CCSD(T)-F12b/aug-cc-pVTZ-PP geometries.

[d] Core correlation effects obtained as difference between all-electron and frozen-core CCSD(T)/aug-cc-pwCVTZ-PP energies at the CCSD(T)-F12b/aug-cc-pVTZ-PP geometries.

[e] Zero-point energy corrections at the CCSD(T)-F12b/aug-cc-pVTZ-PP level of theory.

[f] Final classical relative energies obtained as aVQZ + ΔCore.

[g] Final adiabatic relative energies obtained as aVQZ + ΔCore + ΔZPE.

Table S2. Harmonic vibrational frequencies (in cm^{-1}) for the stationary points of the FCH_3I^- system obtained at CCSD(T)-F12b/aug-cc-pVDZ-PP (aVDZ) and CCSD(T)-F12b/aug-cc-pVTZ-PP (aVTZ) as well as by using the analytical potential energy surface (PES)

	HMIN			TS1			MIN2			TS2		
	aVDZ	aVTZ	PES	aVDZ	aVTZ	PES	aVDZ	aVTZ	PES	aVDZ	aVTZ	PES
ω_1	75	74	69	89i	93i	22	48	49	18	79i	73i	234i
ω_2	290	290	265	69	76	93	62	60	91	63i	51i	176i
ω_3	313	305	286	132	131	159	147	147	158	116	120	152
ω_4	505	502	520	369	371	343	371	373	347	349	352	340
ω_5	942	939	961	461	455	473	601	613	471	382	415	371
ω_6	946	945	981	565	576	545	639	646	532	407	437	513
ω_7	1348	1347	1362	945	943	1016	953	952	1016	930	930	1048
ω_8	1461	1462	1521	958	959	1087	965	965	1081	962	965	1219
ω_9	1517	1521	1548	1365	1366	1467	1367	1367	1465	1365	1364	1614
ω_{10}	2396	2391	2369	2884	2890	2835	2883	2889	2839	2879	2885	2797
ω_{11}	3091	3096	3117	2955	2960	2938	2953	2959	2939	2949	2955	2832
ω_{12}	3155	3162	3173	3778	3772	3789	3643	3633	3800	3874	3858	3841
	MIN3			TS1’			MIN2’			TS2’		
	aVDZ	aVTZ	PES	aVDZ	aVTZ	PES	aVDZ	aVTZ	PES	aVDZ	aVTZ	PES
ω_1	45	45	64	132i	128i	234i	61	55	54	104i	108i	95i
ω_2	90	78	132	139	136	176i	202	198	189	132	129	113
ω_3	151	152	140	141	142	152	376	367	271	144	132	157
ω_4	370	372	352	403	413	340	404	404	426	350	346	382
ω_5	616	628	571	450	452	371	654	657	538	396	398	473
ω_6	651	663	621	531	531	513	675	678	655	550	564	494
ω_7	951	951	1064	936	934	1048	897	893	1014	956	954	1088
ω_8	964	966	1125	1014	1009	1219	948	944	1128	974	972	1114
ω_9	1368	1367	1512	1415	1412	1614	1371	1370	1650	1363	1362	1562
ω_{10}	2889	2895	2890	2843	2847	2797	2904	2908	2897	2886	2892	2941
ω_{11}	2959	2965	3026	2917	2922	2832	3000	3004	2962	2959	2965	3019
ω_{12}	3601	3591	3673	3816	3811	3841	3576	3577	3658	3794	3787	3843
	FSMIN			PREMIN			POSTMIN			HTS		
	aVDZ	aVTZ	PES	aVDZ	aVTZ	PES	aVDZ	aVTZ	PES	aVDZ	aVTZ	PES
ω_1	146	146	131	111	121	83i	75	73	46	113i	112i	118i
ω_2	150	147	131	112	122	149	85	79	46	112	115	100
ω_3	273	274	260	162	155	149	87	86	75	174	174	165
ω_4	478	477	496	331	299	256	1004	999	999	447	444	458
ω_5	802	794	791	847	849	919	1173	1171	1200	763	761	790
ω_6	803	795	791	847	849	919	1173	1171	1200	886	885	920
ω_7	1213	1207	1272	1139	1130	1120	1451	1455	1471	1186	1189	1204
ω_8	1470	1472	1513	1431	1433	1480	1494	1498	1512	1439	1443	1500
ω_9	1471	1473	1513	1431	1433	1480	1494	1498	1512	1452	1453	1504
ω_{10}	3024	3024	3086	3156	3159	3177	3076	3077	3081	3115	3112	3129
ω_{11}	3113	3116	3149	3299	3306	3343	3178	3180	3185	3243	3240	3259
ω_{12}	3114	3116	3149	3299	3306	3343	3178	3180	3185	3245	3245	3273
	DITS			WALDENTS			FSTS					
	aVDZ	aVTZ	PES	aVDZ	aVTZ	PES	aVDZ	aVTZ	PES			
ω_1	765i	767i	775i	273i	231i	206i	599i	591i	582i			
ω_2	76	79	81	169	166	166	78	37i	112			
ω_3	286	285	297	170	166	166	164	164	176			
ω_4	361	354	316	226	226	239	402	401	400			
ω_5	558	555	553	875	871	927	830	824	820			
ω_6	850	845	874	875	871	927	842	838	962			
ω_7	976	982	977	1075	1083	1107	1144	1150	1219			
ω_8	983	984	986	1417	1422	1477	1418	1421	1427			
ω_9	1305	1301	1358	1417	1422	1477	1478	1482	1566			
ω_{10}	2824	2828	2632	3175	3173	3176	3090	3090	3007			
ω_{11}	3150	3151	3121	3346	3340	3348	3195	3197	3239			
ω_{12}	3307	3308	3296	3346	3341	3348	3253	3254	3254			

Table S3. Harmonic vibrational frequencies (in cm^{-1}) for the reactant and main product channels of the $F^- + CH_3I$ reaction obtained at CCSD(T)-F12b/aug-cc-pVDZ-PP (aVDZ) and CCSD(T)-F12b/aug-cc-pVTZ-PP (aVTZ) as well as by using the analytical potential energy surface (PES)

	CH_3I			CH_3F			CH_2I^-			HF		
	aVDZ	aVTZ	PES	aVDZ	aVTZ	PES	aVDZ	aVTZ	PES	aVDZ	aVTZ	PES
ω_1	552	549	550	1083	1077	1110	373	374	386	4151	4143	4110
ω_2	902	899	922	1207	1206	1195	945	944	983			
ω_3	903	899	922	1207	1206	1195	952	952	1030			
ω_4	1289	1287	1275	1492	1495	1500	1363	1363	1460			
ω_5	1475	1479	1468	1505	1509	1567	2876	2880	2863			
ω_6	1475	1479	1468	1505	1510	1567	2945	2950	2954			
ω_7	3087	3087	3088	3047	3050	3069						
ω_8	3199	3201	3224	3137	3141	3129						
ω_9	3199	3201	3224	3137	3141	3129						

Table S4. $Q[v,b]$ direct/indirect trajectory separation function (Eq. S1) parameters at different collision energies (see Figure S5)

Parameter	Collision energy (kcal/mol)						
	1.0	4.0	7.4	10.0	15.9	35.3	50.0
r_0 (ps)	2.94E−03	2.64E−01	−2.78E−02	−1.33E−02	−3.14E−02	−1.13E−01	−1.30E−01
r_1 (ps/bohr)	3.89E−02	1.38E−02	−1.00E−02	−5.86E−03	−1.75E−02	1.85E−03	5.59E−02
r_2 (ps/bohr^2)	−6.31E−03	3.26E−04	1.17E−02	1.52E−02	1.98E−02	1.78E−03	−2.97E−02
r_3 (ps/bohr^3)	5.46E−04	2.20E−04	−3.57E−04	−6.44E−04	−1.27E−03	2.23E−03	7.77E−03
r_4 (ps/bohr^4)	−6.45E−06	−4.41E−06	4.65E−07	1.01E−05	2.80E−05	−1.33E−04	−4.06E−04
s_0 (ps)	2.45E+00	1.09E+00	1.09E+00	5.32E−01	5.32E−01	5.32E−01	5.32E−01
s_1 (ps)	4.12E+00	2.41E+00	2.41E+00	9.47E−01	9.47E−01	9.47E−01	9.47E−01
s_2 (m/s)	1.51E+02	1.54E+02	1.54E+02	2.11E+02	2.11E+02	2.11E+02	2.11E+02

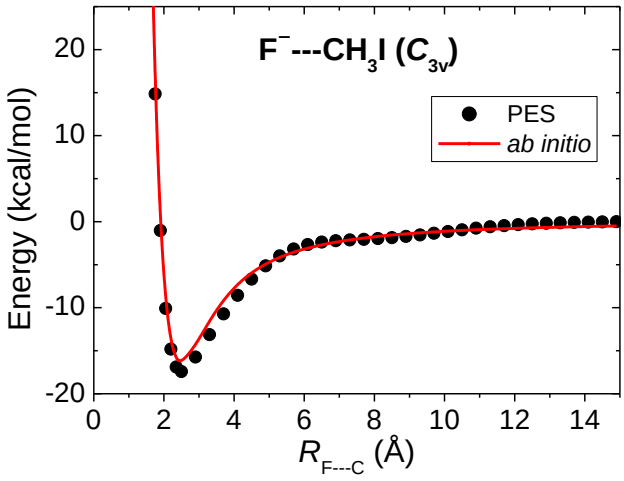

Figure S1. Potential energy curves obtained from the analytical PES and direct *ab initio* computations at the CCSD(T)-F12b/aug-cc-pVTZ-PP + ΔCore[CCSD(T)/aug-cc-pwCVDZ-PP] level of theory as a function of the F···C distance along the C_3 axis of $F^-\cdots CH_3I$(eq.).

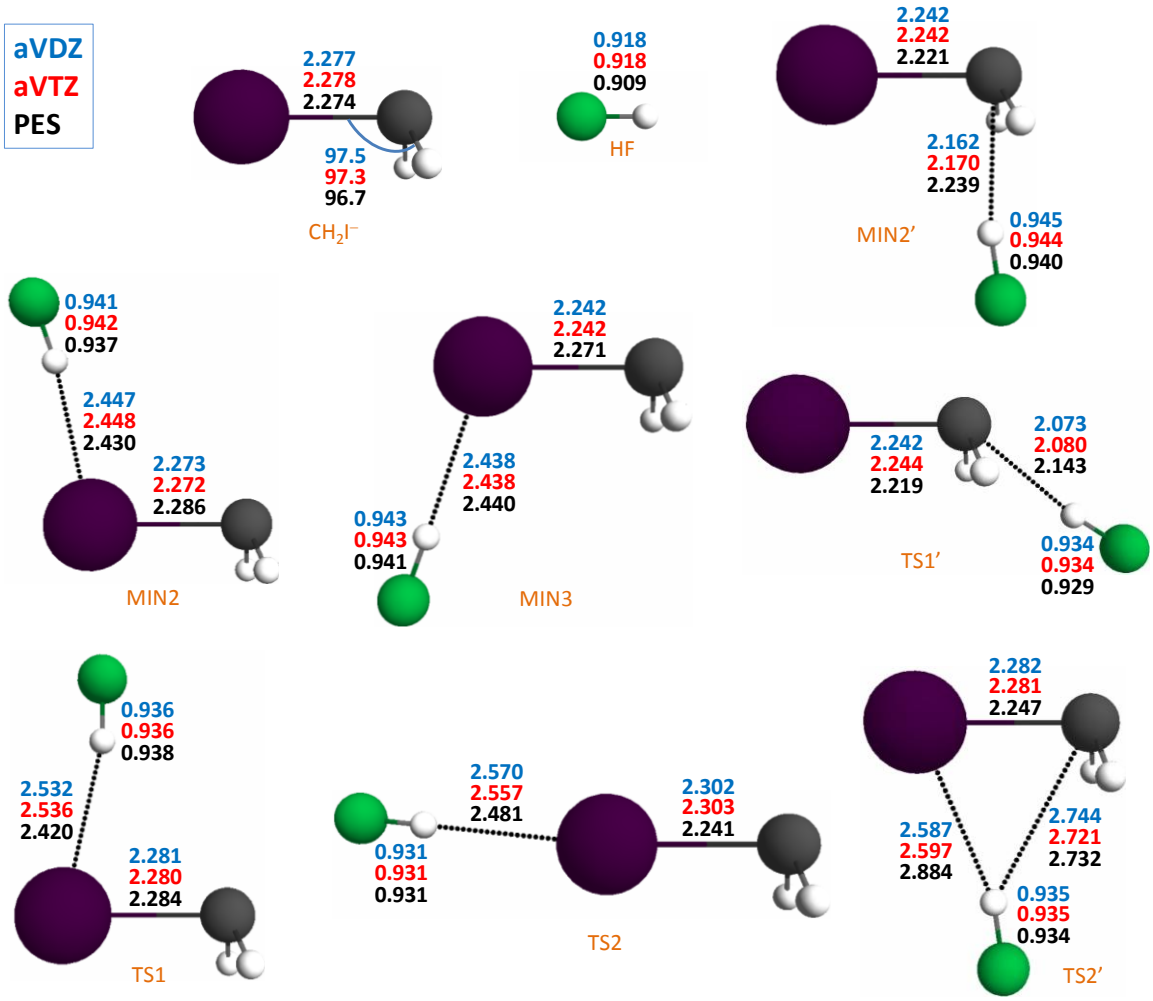

Figure S2. Stationary-point structures corresponding to the abstraction channel of the $F^- + CH_3I$ reaction showing the representative structural parameters (distance in Å and angles in degrees) obtained at CCSD(T)-F12b/aug-cc-pVDZ-PP (aVDZ) and CCSD(T)-F12b/aug-cc-pVTZ-PP (aVTZ) as well as by using the analytical potential energy surface (PES).

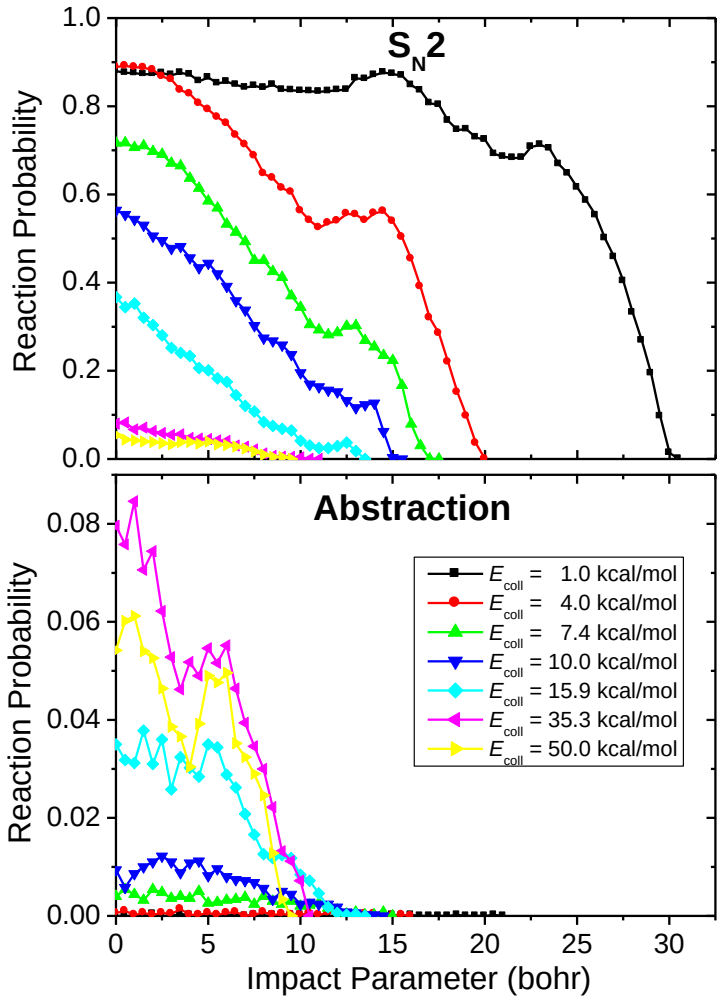

Figure S3. Reaction probabilities as a function of impact parameters for the S_N2 and abstraction channels of the $F^- + CH_3I$ reaction at different collision energies.

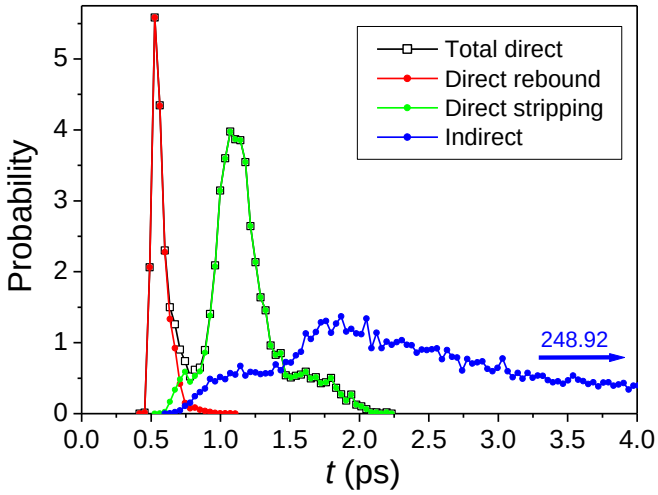

Figure S4. Mechanism-specific trajectory integration time distributions for the F^- + CH_3I S_N2 reaction at collision energy of 10 kcal/mol.

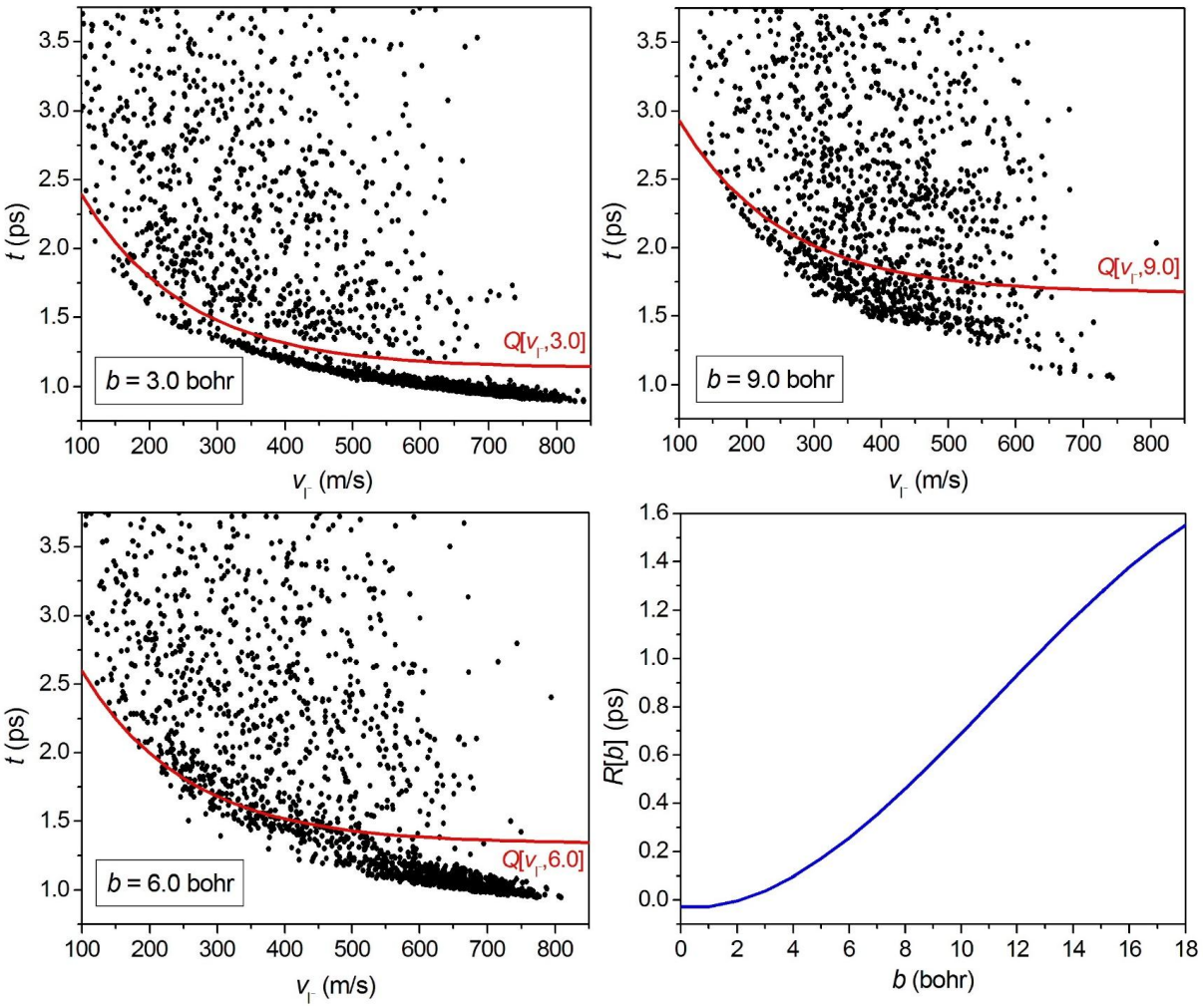

Figure S5. Representative trajectory integration time (t) *vs.* leaving group velocity (v) distributions for b = 3, 6, and 9 bohr at a collision energy of 7.4 kcal/mol. The direct and indirect trajectories at a given collision energy are distinguished based on the $Q[v,b]$ separation function written as a sum of the univariate functions $S[v]$ and $R[b]$ as

$$Q[v,b] = R[b] + S[v] = r_0 + r_1 b + r_2 b^2 + r_3 b^3 + r_4 b^4 + s_0 + s_1 e^{-\frac{v}{s_2}}. \qquad \text{(S1)}$$

Accordingly, below and above the $Q[v,b]$ function (red lines) are the direct and indirect trajectories, respectively, whereas the $R[b]$ function (blue line) incorporates the impact parameter (b) dependence of the separation function. All the function parameters, which define the above functions, are given in Table S4 at each collision energy. The rebound (backward scattered, $\theta > 90°$) and stripping (forward scattered, $\theta < 90°$) direct trajectories are separated based on their scattering angles (θ) as indicated.

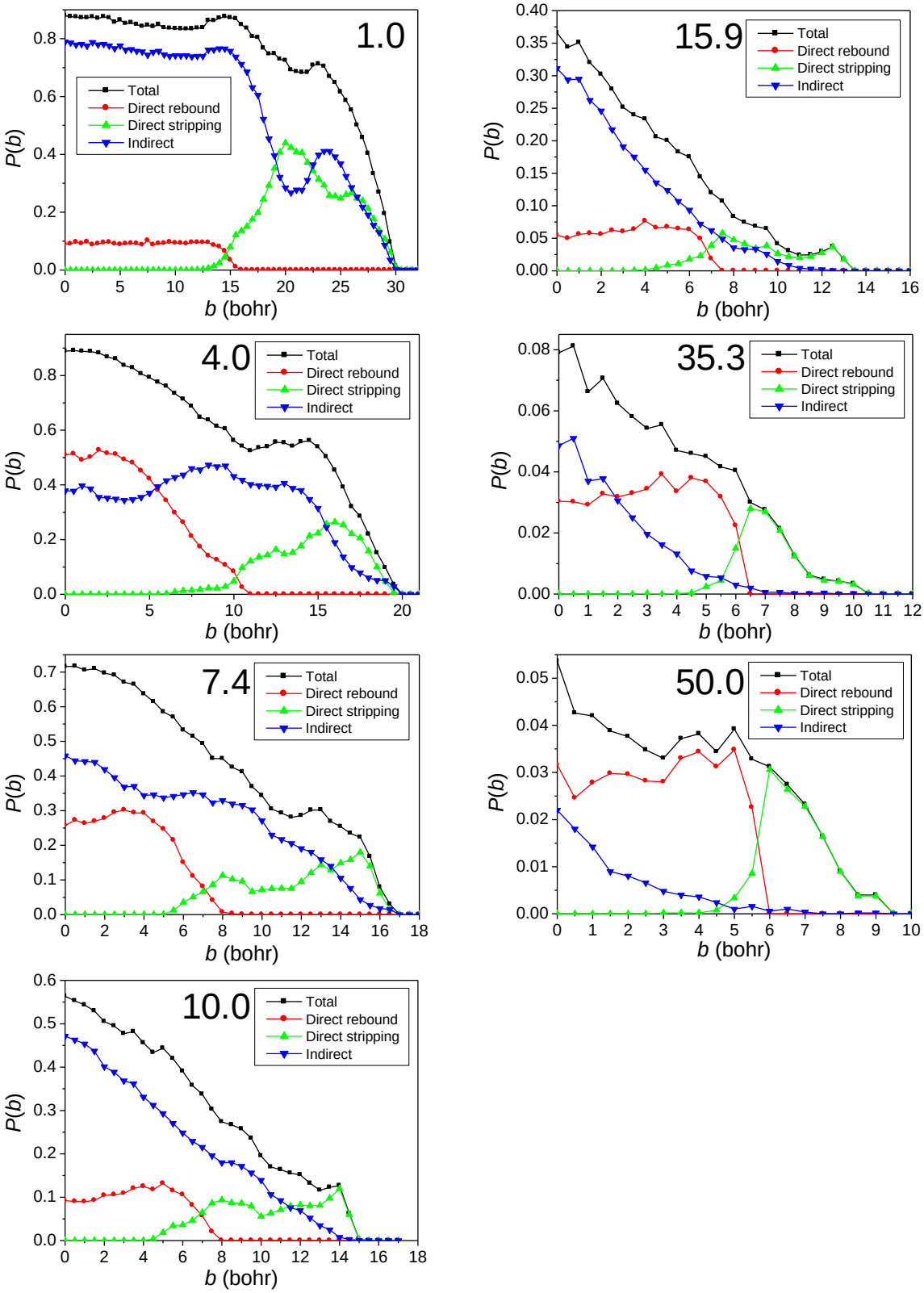

Figure S6. Mechanism-specific reaction probabilities as a function of impact parameters for the $F^- + CH_3I$ S_N2 reaction at different collision energies (as indicated in kcal/mol).